Radiation Protection Dosimetry (2020), Vol. 190, No. 2, pp. 125–131 doi:10.1093/rpd/ncaa085
Advance Access publication 1 July 2020

MEASUREMENT AND ANALYSIS OF THE NEUTRON ENERGY SPECTRUM AND ASSOCIATED OCCUPATIONAL EXPOSURE FROM A SHIELDED ^{241}AM-BE SOURCE

Jimmy Steele Stringer[1,*], Henry Spitz[1] and Samuel Glover[2]
[1]College of Engineering and Applied Science, University of Cincinnati, 598 Rhodes Hall, P.O. Box 210072, Cincinnati, OH, 45221-0072, USA
[2]National Institute for Occupational Health and Safety Health Effects Laboratory Division, 4676 Columbia Parkway, Cincinnati, OH, 45226, USA

*Corresponding author: stringjy@mail.uc.edu; jimmy.sstringer@gmail.com

Received 16 October 2019; revised 11 February 2020; editorial decision 25 March 2020; accepted 25 March 2020

A set of five Bonner spheres was used to measure the ambient neutron H*(10) dose around an orphan ^{241}Am-Be neutron source shielded with different arrangements and types of neutron-absorbing materials. These results were compared to measurements obtained using a portable radiation dosemeter. The Bonner sphere measurement results identified the presence of a large thermal and intermediate neutron component from the shielded ^{241}Am-Be source that was not revealed using the portable instrument.

INTRODUCTION

The dose received by workers from neutron exposure is highly dependent on the neutron energy spectrum emitted by the source. The complexity of neutron spectroscopy is compounded by the fact that interaction probabilities vary significantly with energy over several orders of magnitude so that detection is typically not possible with a single detector. Although mathematical simulation and Monte Carlo analysis can be used to predict the neutron energy spectrum, validation of the predicted energy spectrum is constrained by the lack of instruments that adequately respond over a wide range of neutron energies. Neutron spectroscopy utilising Bonner spheres was introduced by Barmblett et al. in 1960[(1)]. These neutron detectors rely on a large neutron moderation assembly surrounding a thermal neutron detector to achieve a known energy response over an energy range from thermal up to 20 MeV[(2)]. Bonner sphere measurements exhibit high detection efficiency, simple operation, isotropic angular response and excellent photon discrimination[(3)]. Although a complex mathematical unfolding process must be applied to the set of measurements, Bonner sphere spectroscopy (BSS) is truly the gold standard for determining neutron energy fluence.

The Ludlum model 42–5 BSS system uses a set of five polyethylene spheres of increasing diameter to moderate fast and intermediate neutrons to thermal energies. A small $Li^6I(Eu)$ scintillation detector is located at the centre of the detection assembly and responds to the energy deposition produced by alpha particles generated in the $Li^6(n,\alpha)He^3$ reaction. The thermal neutron absorption cross-section for Li^6 is 941 barns and includes a $Li^6(n,\alpha)He^3$ resonance for thermal neutron interactions, which generates a 4.78 MeV photon[(4)].

$$Li_3^6 + n_0^1 \rightarrow H_1^3 + \alpha_2^4 + 4.78\ MeV \tag{1}$$

Depending upon radius, each Bonner sphere differentially moderates to thermal energy a portion of the neutron energy spectrum emitted by the source. Analysis of the relative response of each of the Bonner sphere detectors with detector radius can reveal information about the actual neutron energy spectrum. This analysis involves solving an integral equation, in which the unknown function representing the neutron energy distribution appears as the integrand. This integral equation is the Fredholm integral (Equation (2)), which can be solved to provide a function that describes the unknown neutron energy fluence, $\phi_E(E)$[(8)],

$$C = \int_{E_i}^{E^f} R_\varphi(E)\varphi_E(E)dE \tag{2}$$

where C represents counts measured with the Bonner sphere, $R_\phi(E)$ is the Bonner sphere response function and $\phi_E(E)$ is the neutron energy fluence. Thus, the number of counts measured by the Bonner sphere system is the convolution of the detector response function and the neutron energy fluence. The discretised Fredholm integral coupled with mathematical optimisation techniques provides a means to obtain an optimal neutron energy spectrum. Dose

can be determined by convolution of the optimal spectrum with energy-dependent dose conversion factors. While BSS is mature and robust, there are underlying issues that may make BSS suboptimal for workplace measurements. For example, the ergonomic design of the BSS is cumbersome and presents a physical challenge for routine workplace measurements[5]. BSS also exhibits a monotonically decreasing energy response for neutrons above 10 MeV, which makes traditional BSS suboptimal for high-energy applications. This under response can be 10 orders of magnitude[6]. A complex deconvolution must be utilised to extract the spectrum in order to compute accurate doses or dose rates. Thus, portable neutron detectors were developed as an alternative to BSS. Commercially available, portable neutron detectors are less cumbersome to use than Bonner spheres but sacrifice accuracy for ease of use. Portable neutron detectors do not measure the neutron energy spectrum but estimate dose using a generalised fluence to dose conversion factor. There are several portable instruments that are currently commercially available. This study used Prescila© (Proton Recoil Scintillator Los Alamos), a dual scintillator system developed by Los Alamos National Laboratory (LANL)[4]. This detection system uses a ZnS (Ag) scintillator for high energy neutron detection and a LiF ZnS (Ag) mixed scintillator for epi-thermal and thermal neutron detection. While this design exhibits a robust response to low and high energy neutrons, it is less responsive to intermediate energy neutrons. The reduced response to epithermal neutrons with Prescila© is addressed by increasing the magnitude of the epi-thermal and thermal neutron response, which creates a correspondingly scaled response to intermediate and fast neutrons[5]. Unfortunately, this adjustment in Prescila© detector response generates an average dose and dose rate error that is reported to be the greatest among the five classes of wide-energy neutron dosemeters that have emerged since 1970[8].

This project used BSS and a Prescila© portable neutron detector to evaluate occupational exposure from an orphan 5 Ci ^{241}Am-Be neutron source that is stored in a neutron transport shielding assembly when not in use (Figure 1). The source is manually removed from the shielding assembly to test and calibrate portable neutron survey instruments. Workers handling the source and occupants of offices surrounding the storage room may receive a small radiation dose whenever the source is used. This paper evaluates the occupational exposure and radiation dose associated with use of this source when it is stored in its shield and when it is removed from the shield during routine use. The location and position of the source during use generate considerable neutron scatter such that the neutron energy spectrum is very complex.

Figure 1. Gamma Industries shipping container.

METHODS

A 5 Curie ^{241}Am-Be source is physically located in the corner of a small, unoccupied storage room with adjacent offices lining its outer walls. The ^{241}Am-Be source is stored inside a Gamma Industries neutron shipping container having an inner liner filled with a super saturated mixture of water and borax (Figure 1). The shipping container is stored inside a box lined with multiple layers of borated polyethylene (Figure 2). Another layer of moderation is provided by nine 5-gallon water-filled pails arranged in a 3 × 3 matrix that shield the front of the polyethylene-lined box (Figure 3).

Neutron detection and unfolding

Neutrons emitted by the ^{241}Am-Be source were measured using the Ludlum model 42–5 BSS with four different arrangements of shielding materials as described in Table 1. A Ludlum Model 2200 scaler/timer recorded counts from the $Li^6I(Eu)$ scintillation detector. Figure 4 shows two arrangements of the source and detector during measurements. The Ludlum model 42–5 BSS includes five individual polyethylene (PE) spheres with diameters ranging from 0 (unmoderated) to 38.1 cm. At the centre of each sphere is a 0.4 cm × 0.4 cm cylindrical $Li^6I(Eu)$ thermal neutron detector that is coupled to a photomultiplier tube. The count rate generated by the $Li^6I(Eu)$ detector was used to create a histogram of the neutron energy flux emitted by the ^{241}Am-Be source. The centre of the detector was positioned

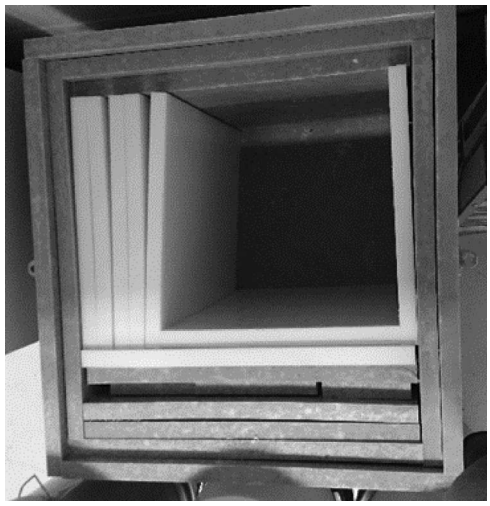

Figure 2. Top view of a box lined with sheets of borated polyethylene in which the shipping container is stored.

Figure 3. Arrangement of nine 5-gallon plastic pails filled with water as moderation for the shielded Am-Be neutron source located behind the pails.

25 cm above the floor at a distance of 100 cm from the central axis of the source. The measurement time was at least 10 min. to achieve a statistical uncertainty of 10% or better. The neutron spectrum was unfolded using the UGM 3.3 code and the BSS detector response matrix provided by the manufacture. The unfolding process utilised an initial estimate of the spectrum as a default for a maximum entropy optimisation method required by the UGM 3.3 code[9].

The Prescila© portable neutron detector was exposed to the same shielded source arrangements as used with the BSS listed in Table 1. Prescila© measures dose rate (mrem/hr) as opposed to integral counts measured by the Ludlum 42–5. The average of five measurements with Priscila© was reported for each of the shielded source arrangements listed in Table 1.

Table 1. Different shielding arrangements for the Am-Be source

Arrangement ID #	Source shielding type
1	None – unshielded
2	Shipping Cask
3	Shipping Cask + PE Lined Box
4	Shipping Cask + PE lined box +Water

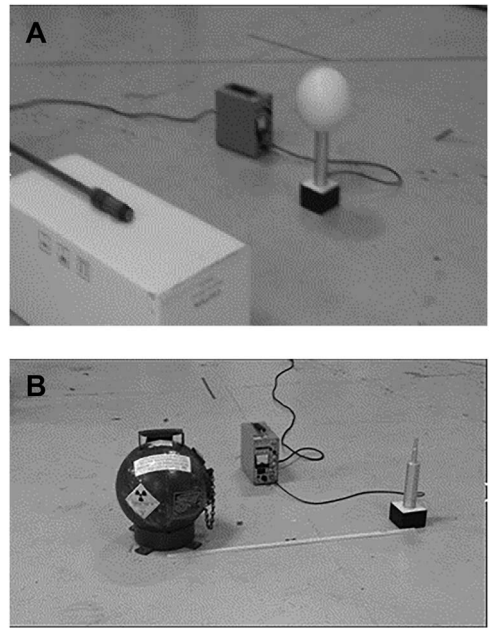

Figure 4. Left: Unshielded ^{241}Am-Be source measured with an x-cm diameter polyurethane moderated Li^{6}I(Eu)detector. Right: Source stored inside shipping cask measured with a bare (unmoderated) Li^{6}I(Eu) detector.

MCNP modeling

The radiation output from the ^{241}Am-Be source was also simulated utilising the Monte Carlo code MCNP6[11] for all source arrangements. Figure 5 illustrates the boundaries and volumes involved with configuration 4 in Table 1. The ^{241}Am-Be source neutron energy spectrum was defined in the simulation according to ISO 8529-1[10]. A deterministic neutron fluence tally using MCNP F5 detectors was used to predict the neutron fluence at a meter away from the unmoderated source (arrangement 1). Predictions from the simulation were compared to the Bonner sphere neutron energy spectrum for an unmoderated source.

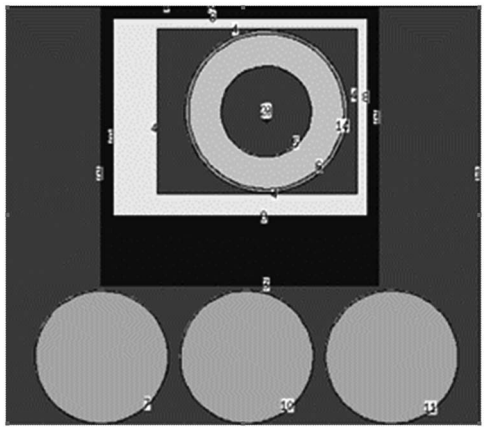

Figure 5. MCNP Source Configuration.

RESULTS

Bonner sphere

Figure 6a shows the energy fluence normalised to the maximum energy determined from the BSS measurements for each shielding arrangement. Figure 6a also illustrates how the relative energy fluence for each energy region changes as shielding is increased. As more moderation is introduced, the height and width of peaks in the thermal and intermediate neutron energy regions increase while the width of the high-energy peaks decrease. Figure 6b–d show details of these changes for the thermal, intermediate and high neutron energy regions, respectively.

Figure 6b shows that the quality (average energy) and quantity (fluence) of scatter in the thermal region increase as more shielding is added. Although arrangement 4 (labeled as water wall in Figure 6b) generated the largest quantity of thermal energy neutrons, the greatest total energy in the thermal region (summed energy fluence) occurred with arrangement 2 (labeled as cask in Figure 6b). The total neutron energy in the thermal region with arrangement 2 was 42% greater than with arrangement 1 (unshielded).

The mean neutron energy generated with shielding arrangements 3 (labeled as box in Figure 6c) and 4 (labeled as water wall in Figure 6c) is shifted lower into the intermediate energy distribution as shown in Figure 6c. Unlike Figure 6b, the mean neutron energies in the intermediate region are not unique suggesting that high neutron energy interactions lead to increased dispersion of energy fluence into the intermediate region. In the intermediate region, the cask shielding configuration 2 has the greatest average energy and total energy.

Figure 6d shows that the greatest neutron energy and summed energy fluence in the high neutron energy region occur with shielding arrangement 1 (unshielded source). The mean energy in the high neutron energy spectrum is about the same for all shielding configurations. However, the total energy decreases as shielding increases.

The neutron energy spectrum determined from BSS analysis was converted to dose using the fluence-to-dose conversion matrix from ICRU report 57[11]. A regression was performed to determine the appropriate fluence to dose conversion equation for the thermal, intermediate and high-energy regions. The units were converted to dose rate (rem per hour) for comparison with measurements using Prescila©. The measured dose rates obtained with Prescila for each configuration listed in Table 2 were all significantly less than the converted dose rate measurements using BSS.

Bonner sphere vs. MCNP spectra

Figure 7 compares the measured and predicted neutron energy spectra for the unshielded (bare) ^{241}Am-Be source (arrangement 1) in which scatter from the floor was intentionally neglected in the simulation. The spectra are normalised to the maximum energy fluence. Figure 8 shows results when the neutron scatter component from the floor is included in the simulation revealing a large peak in the thermal region. Unfortunately, this component is not observed by measurement since the position of the $Li^6I(Eu)$ detector assembly 25 cm from the floor effectively reduces the fraction of neutrons entering the moderator that have been scattered from the floor. Thus, the solid angle created by the position of the $Li^6I(Eu)$ detector reduces the sensitivity of the detector to neutrons scattered from the floor.

The relative response of the each of the Bonner spheres with Prescila, normalised to the unmoderated bare source (configuration 1) for each of the three remaining source configurations, is shown on Figure 9. Since the energy fluence changes with the source shielding configuration, Figure 9 demonstrates that the relative energy response of Prescila is most similar to the 38.1 cm Bonner sphere.

DISCUSSION

The normalised energy fluence measured using the BSS for each shielding arrangement was estimated using a Riemann sums analysis to calculate the total area under each curve in Figure 6a. The neutron energy fluence from the unshielded source (arrangement 1) can be reduced by 50% using the shipping cask alone (arrangement 2). The reduction is increased to 73% by surrounding the shipping cask with the polyethylene box (arrangement 3). The combination of the shipping cask, polyethylene box, and water pails (arrangement 4) reduces the

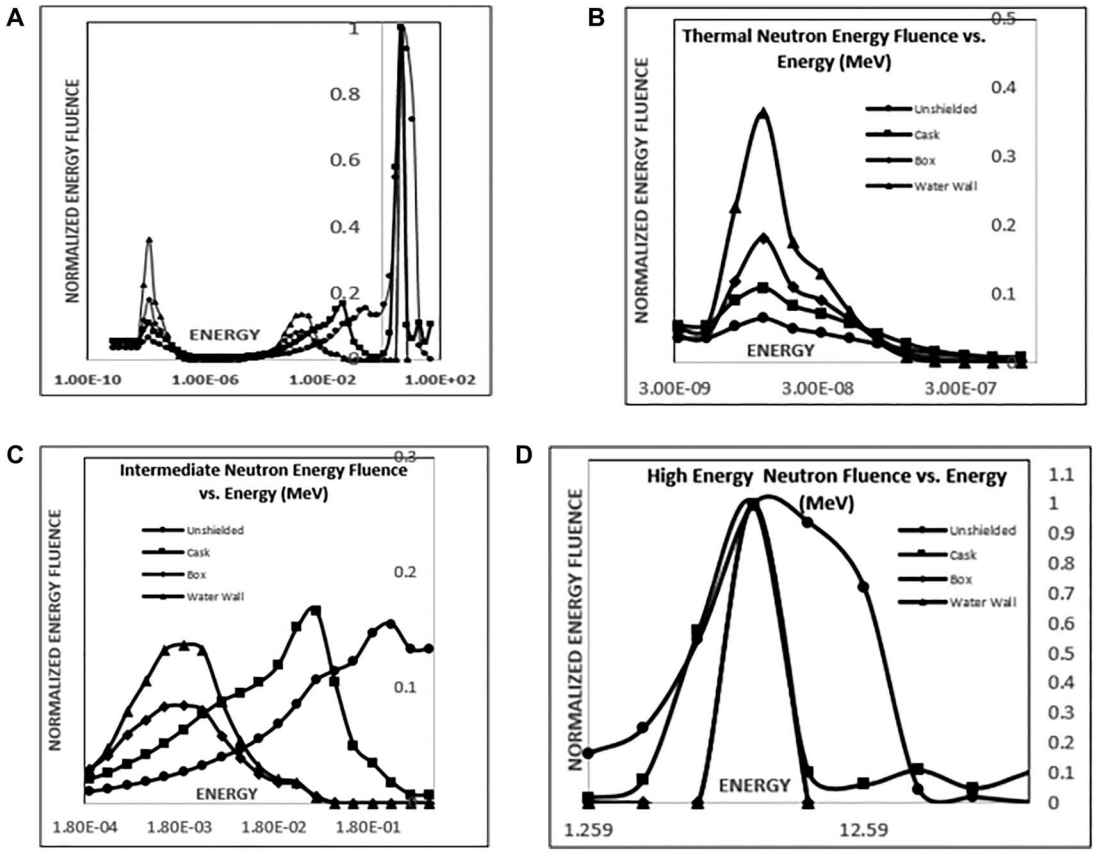

Figure 6. (**a**) Bonner sphere normalised energy fluence for each shielding arrangement. ■ Shipping Cask, ♦ Shipping Cask + PE Lined Box ▲ Shipping Cask + PE lined box + Water • Unshielded Source □. (**b**) BSS measured thermal neutron energy fluence vs. energy for different shielding arrangements. (**c**) BSS measured intermediate neutron energy fluence vs. energy for different shielding arrangements. (**d**) BSS measured high neutron energy fluence vs. energy for different shielding arrangements. Comparison of dose rate determined using BSS and Prescila©.

neutron energy fluence by 83% compared to the unshielded source. Applying the ICRP fluence-to-dose conversion factors to the neutron energy fluence estimated for each shielding arrangement, the reduction in dose is 34%, 43.1%, and 45% for arrangements 2, 3, and 4, respectively The same analysis was performed using results measured with Prescila© revealing a dose reduction of 39%, 50.4% and 52.4% for arrangements 2, 3 and 4, respectively. While measurements of the neutron energy fluence determined using Prescila© and the BSS for each shielding arrangement were similar, the absolute dose determined using Prescila© was consistently lower than the dose determined using the BSS. Table 2 shows that the dose rates for each shielding arrangement determined using BSS were consistently twice that measured using Prescila©. This bias may be related to the limited response of Prescila© in the intermediate region of the neutron energy spectrum.

Table 2. Dose rate comparison for different shielding configurations

Configuration	Bonner sphere (rem hr^{-1})	Prescila© (rem hr-)
1	37.4	17.9
2	12.9	5.9
3	3.41	1.46
4	0.745	0.352

Figure 9 shows the relative energy response for all systems. The response of Prescila© is similar to the 38.1 cm Bonner sphere except at the thermal and intermediate range of neutron energy where the instrument under responds. Use of Prescila© to monitor exposure in the presence of a complex

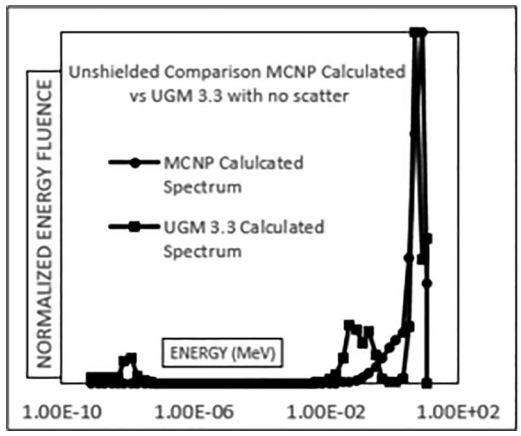

Figure 7. Comparison of the normalised neutron energy spectrum measured and predicted from an unmoderated Am-Be source. Scatter from the floor was intentionally neglected in this simulation.

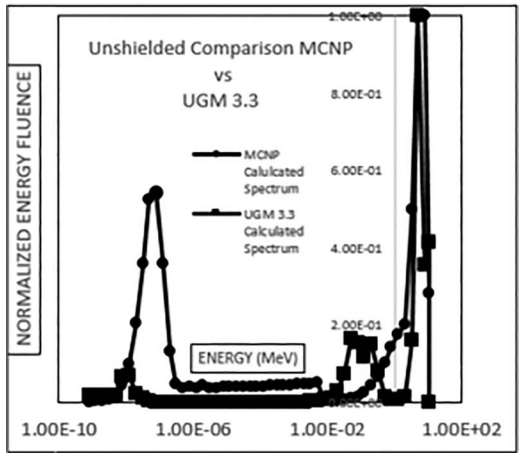

Figure 8. Comparison of the normalised neutron energy spectrum measured and predicted from an unmoderated ^{241}Am-Be source. The large peak in the thermal region is due to scatter from the floor.

neutron energy spectrum having an abundance of thermal and intermediate energy neutrons could lead to an underestimate of the dose to workers[7].

Comparing the simulated neutron energy spectrum with the unfolded BSS spectrum shows the significance of the scattered thermal neutron energy component when the ^{241}Am-Be source is used. Although all the BSS moderators are spherical in shape, the BSS does not exhibit a true 4π response in use because of the position of the $Li^6I(Eu)$

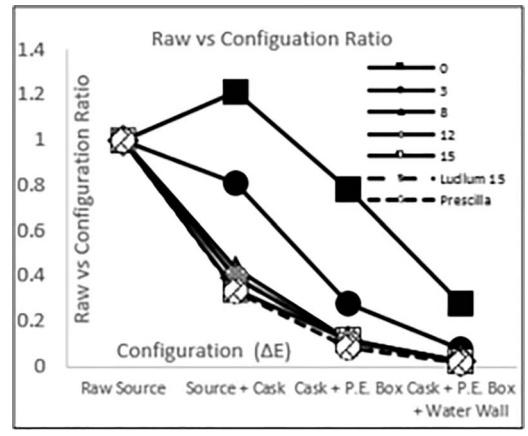

Figure 9. Ratio of unmoderated (configuration 1) to moderate response (Configurations 2–4) measured using BSS and Prescila.

scintillation detector in the spherical moderator, relative to floor scatter. Thus, neutrons scattered towards the detector from the floor below the detector are obscured. The importance of the scattered neutron component from the floor to the simulated thermal neutron energy fluence was also recognised when the floor was omitted as a surface in the Monte Carlo simulation.

The higher energy regions of the neutron energy spectrum are relatively less affected by room scatter as compared to the thermal region in the model.

CONCLUSION

The key to accurate workplace neutron dosimetry is having knowledge about the neutron energy spectrum and understanding how the monitoring instruments detect neutrons. During use of the ^{241}Am-Be source, workers are exposed to a large thermal and intermediate neutron spectral component. The dose measured using the BSS was nearly twice that measured using Prescila©. The Monte Carlo simulation revealed a larger thermal and intermediate neutron component than BSS could detect, underscoring the need for a well-characterised neutron energy spectrum for accurate neutron dosimetry.

DISCLAIMER

The findings and conclusions in this report are those of the authors and do not necessarily represent the official position of the National Institute for Occupational Safety and Health, Centers for Disease Control and Prevention.

REFERENCES

1. Bramblett, R. L., Ewing, R. I. and Bonner, T. W. *A new type of neutron spectrometer*. Nucl. Inst. And Meth. **9**, 1–12 (1960).
2. Kralik, M., Aroua, A., Grecescu, M., Mares, V., Novotný, T., Schraube, H. and Wiegel, B. *Specification of Bonner sphere systems for neutron spectrometry*. Radiat. Prot. Dosimetry **70**, 279–284 (1997).
3. Chu, M. C., Fung, K. Y., Kwok, T., Leung, J. K. C., Lin, Y. C., Liu, H., Luk, K. B., Ngai, H. Y., Pun, C. S. J. and Wong, H. L. H. *Development of a Bonner sphere neutron spectrometer from a commercial neutron dosimeter*. J. Instrum. **11**(11), 2 (2016).
4. Wehe, D. K. and Knoll, G. F. *Chapter 15 Detectors Based on Fast Neutron-Induced Reactions. Radiation Detection and Measurement, Solutions Manual*, 4th edn. (Hoboken: John Wiley & Sons, Inc) (2012).
5. Olsher, R. H., Seagraves, D. T., Eisele, S. L., Bjork, C. W., Martinez, W. A., Romero, L. L., Mallett, M. W., Duran, M. A. and Hurlbut, C. R. *Prescila: a new, lightweight neutron rem meter*. Health Phys. **86**(6), 603–612 (2004). doi: 10.1097/00004032-200406000-00005.
6. Wiegel, B. *et al. Intercomparison of radiation protection devices in a high-energy stray neutron field, part II: Bonner sphere spectrometry*. Radiat. Meas. **44**(7–8), 660–672 (2009). doi: 10.1016/j.radmeas.2009..03.026.
7. Thomas, D. J. and Klein, H. *Neutron spectroscopy hand book*. Radiat. Prot. Dosim. **107**, 23–33 (2003).
8. Oakes, T. M. *An accurate and portable solid state neutron rem meter*. Nucl. Inst. And Meth. A **719**, 6–12 (2013).
9. Reginatto, M., Goldhagen, P. and Neumann, S. *Spectrum unfolding, sensitivity analysis and propagation of uncertainties with the maximum entropy deconvolution code MAXED*. Nucl. Instr. Meth. A **476**, 242–246 (2002).
10. ISO - International Organization for Standardization. ISO 8529-1:2001 - Reference Neutron Radiations – Part 1: Characteristics and Methods of Production, 15 June 2017, www.iso.org/iso/catalogue_detail.htm?csnumber=25666.
11. 4. Conversion Coefficients. Journal of the International Commission on Radiation Units and Measurements, **os29**(2) (1998). doi: 10.1093/jicru/os29.2.22.